Application of a surface-applied cathodic protection system on a light weight concrete bridge – Part I: Condition assessment, intervention options and trial investigations

J. Gulikers
Ministry of Infrastructure and The Environment, Rijkswaterstaat-GPO, Utrecht, Netherlands
R. Giorgini
CorrPre Engineering, Reeuwijk, Netherlands
A.J. van den Hondel
Vogel Cathodic Protection, Zwijndrecht, Netherlands

ABSTRACT: During regular inspections performed in 2011 a significant amount of hollow-sounding areas were detected over the full length of a cantilever of a box girder bridge. Being the first in a triptych, this paper will discuss the investigations that were performed for condition assessment, the evaluation of the results obtained, and the available practical options to bring the structure in an acceptable serviceable condition. Finally, the solution considered to be the most economical and practical, i.e. the application of galvanic cathodic protection, is described in more detail.

1 INTRODUCTION

During regular inspections performed in 2011 a significant amount of hollow-sounding areas were detected over the full length of a cantilever of a box girder bridge. In the first inspection report the cause was described as 'unknown'. This situation resulted in a number of detailed technical inspections in order to assess the nature, extent and cause of these hollow areas. The information thus obtained would help in the decision process on the measures to be taken for effective and efficient long-term management.

This paper constitutes part 1 of a triptych which will mainly focus on the condition assessment of the bridge, discuss the possible methods of intervention and provide details on the trial exercise with the proposed galvanic cathodic protection. Part 2 addresses practical issues regarding the execution of the galvanic protection system whereas Part 3 discusses in more detail the issue of the so-called throwing power.

2 DESCRIPTION OF THE BRIDGE

The Neerbossche bridge built in 1982 is located west of Nijmegen and spans the Maas-Waal canal. The structure consists of two twin bridges, referred to as the northern and the southern bridge, see Figure 1 for a cross section and major dimensions. Both box girder bridges are post-tensioned in the longitudinal direction with the main span composed of 31 lightweight concrete segments of 3.40m length. In the horizontal part of the cantilevers 6 post-tensioned steel cables are employed as transverse prestressing. The low-density concrete for the segments was achieved using expanded clay as lightweight aggregate.

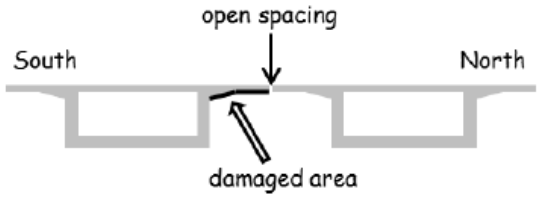

Figure 1. Cross section of the Neerbossche bridge indicating the damaged area and the open spacing between the northern and southern bridge.

In compliance with the then prevailing codes (VB 1974) the required minimum cover depth to the reinforcing steel for structural slab-like elements exposed to aggressive exposure conditions amounted to 25mm. However, for lightweight concrete /structures the minimum cover depth should amount to at least 35mm. It should be noted that at that time, i.e. 1982, the design service life was not explicitly specified in terms of years.

Between both bridges an open spacing of 60mm width is present over the full length. The detailing of this spacing is such that run-off water will flow to the underside of the cantilever of the southern bridge whereas the underside of the northern bridge is sheltered from rain and run-off water by a precast concrete element attached to the deck of the northern bridge. A detailed sketch of the spacing is shown in Figure 2.

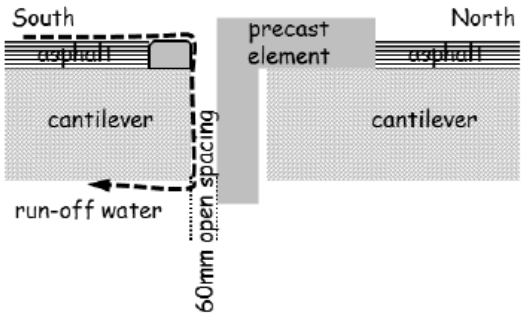

Figure 2. Detail of the open spacing between the northern and southern bridge

A regular condition assessment in 2011, i.e. at an age of 29 years, performed by visual inspection revealed the presence of large areas of delaminated concrete cover at the soffit of one of the cantilevers of the southern bridge. In view of the possible adverse consequences regarding load-bearing capacity, and taking into account the relatively young age, the local authority of Rijkswaterstaat considered it wise to execute more in-depth investigations in the short term to assess the nature and extent of the damage, as well as to find the major cause in order to develop the most economical and effective maintenance strategy for the next decades.

3 TECHNICAL INSPECTIONS

As the visual inspection in 2011 had identified the presence of significant tracks of leakage and taking into account the frequent use of de-icing salts during winter periods, it was likely that chloride-induced corrosion of the reinforcement steel was the primary cause of the extensive delamination observed on the soffit of the southern bridge. Thereupon, in September-October 2012 additional inspections (Boutz 2012a, 2012b and 2012c) were performed to find factual evidence for this reasoning. Stages 1 and 3 were focused on the condition of the soffit of the bridge, whereas in stage 2 the condition of the top side of the bridge deck was assessed. These investigations involved both destructive and non-destructive methods aimed at the detection of areas suspected of reinforcement corrosion.

For the bridge soffit, half-cell potential mapping and electrical resistance measurements were employed to detect corroding spots and areas with high moisture content, respectively. Numerous spots in the cantilever suspect of corrosion could thus be identified whereas the resistance measurements clearly indicated that large concrete areas were very moist.

At several suspect locations the cover was chipped off as to have a visual impression on the nature and depth of the corrosion attack. The appearance of the pits was considered characteristic for chloride-induced reinforcement corrosion.

In addition, a limited number of powder samples were taken so as to quantify the chloride profiles and in particular the chloride content at the level of the reinforcing steel. The results obtained revealed the presence of chlorides with contents ranging from insignificant to values far in excess of 1% (by mass of cement). Figure 3 shows the significant variation in chloride profiles obtained on the bridge soffit (Boutz 2012a, Boutz 2012b, Boutz 2012c).

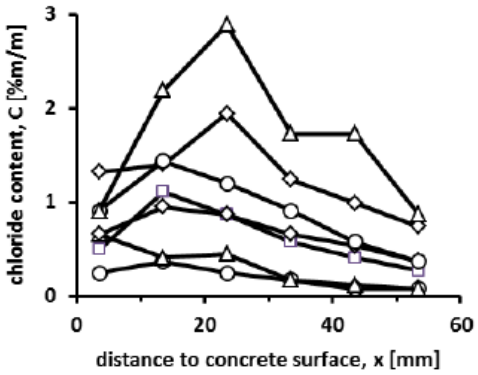

Figure 3. Variation in chloride profiles measured in the bridge soffit.

In order to have a reliable estimate on the concrete surface area to be repaired, the delaminated concrete surface area was approximated by tapping, see Figure 4. The total surface area thus characterised to be delaminated added up to 44m^2.

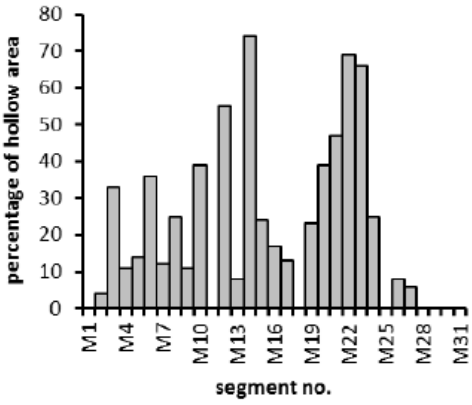

Figure 4. Percentage of delaminated surface area per segment.

In view of the relatively young age of this bridge, the poor accessibility and the localised nature of the damage, the local asset owner asked for an effective and durable solution for at least 25 years, preferably maintenance-free. With this objective and boundary conditions in mind several intervention methods were evaluated.

4 INTERVENTION OPTIONS

In view of the poor accessibility the local asset owner imposed a largely maintenance-free service life of 25 years. In addition, the original dimensions of the bridge had to be maintained not only due to aesthetical reasons but also to prevent an increase of dead weight resulting in discussions on the load bearing capacity.

For all parties involved it was evident from the beginning that, independent of the eventual solution to be chosen, it was essential to eliminate the prime source of chloride contamination of the soffit. This would be achieved simply by closing the open spacing between the two parallel bridges preventing access of run-off water from the bridge deck. In addition, it was clear that any spalled and loose concrete surface areas had to be repaired.

The least invasive and most economical option, at least in the short term, is not to intervene and adopt a "wait and see" approach until significant damage has occurred warranting the need for intervention. However, in the longer term this approach may result in an uncontrolled situation as most of the corrosion attack may proceed largely unnoticed for visual inspection, particularly when bearing in mind that inspection will have to be performed at a large distance, i.e. from the banks of the canal using binoculars. In addition, it was noted that, over time, significant loss of both steel and concrete cross sectional area may develop, leading to an unacceptable risk regarding structural safety. This risk was considered high since chloride penetration in 2011 had already advanced locally to depths beyond the embedded reinforcing steel.

Thus the major task to be addressed in all repair options would be to inhibit the corrosion process already taking place and, in addition, how to prevent future depassivation of the reinforcing steel. The latter problem was considered realistic in view of the significant amounts of chloride that were already present in the cover zone and beyond. Although exposure to external chlorides was virtually impossible after having closed the spacing, redistribution of penetrated chlorides in the undamaged areas could possibly result in an increase of the chloride content at the level of the steel reinforcement in the course of time, in excess of the critical chloride content. Moreover, it was acknowledged that there is a future risk of reinforcement corrosion developing in concrete adjacent to the patched areas due to potential differences arising from repassivation of the steel in the repaired areas. Due to this formation of incipient anodes, patch repairing is not usually adequate to stop further deterioration in the presence of chloride attack (Broomfield, 1997).

A simple, practical and relatively cheap solution would be to replace all spalled and loose concrete areas by repair mortar or shotcrete, thereby restoring passivity. In order to lower the corrosion rate, in addition a hydrophobic treatment or a coating should have to be applied on the complete concrete surface to prevent the concrete to be in direct contact with running water. As a result, the moisture content of the cover zone will gradually decrease to such an extent that the electrolytic pathway in the corrosion circuit will prove to be too resistive to sustain the corrosion process to an appreciable rate. However, it may take more than a decade to achieve such a 'dry' situation and meanwhile corrosion may still proceed at a significant rate. As porous lightweight aggregates have been used in the concrete mix it is likely that a significant amount of water will be contained in the aggregate particles acting as a water reservoir. In addition, the top surface of the bridge deck may show to be the weakest link regarding water ingress. For this option it is therefore essential to waterproof the deck surface to prevent rapid ingress of water by capillary suction. With respect to long-term cost it has to be borne in mind that both hydrophobic treatment and coating have to be re-applied every 5 to 10 years (Christodoulou et al.2014, Dai et al. 2010). Taking into account the fact that the soffit of the bridge is sheltered from direct rain, snow and hail and that the spacing between the bridges will be closed, the application of neither a coating nor a hydrophobic treatment is considered to have any beneficial effect.

A further non-invasive measure in combination with patch repair was to apply a so-called migrating corrosion inhibitor on the concrete surface. This chemical agent is expected to penetrate the concrete cover and upon reaching the reinforcing steel it will intervene in the electrochemical reactions of the corrosion process. However, the effectiveness of such surface-applied inhibitors has not yet been proven to work in practice, particularly in the long term. At present no reliable, preferably non-destructive, method is available to clearly demonstrate on site that inhibitors will result in a significant reduction of the corrosion rate in real structures (Ormellese et al. 2006, Söylev et al., 2007). Moreover, if such a method would be available, it would necessitate frequent monitoring and inevitably lead to additional cost.

The most drastic option was to remove all chloride-contaminated concrete and replace this by shotcrete. However, taking into account the observed chloride penetration depth, this would imply that over large areas, the concrete cross section of the cantilever would be significantly reduced. Due to this temporary reduction it was anticipated that the load-bearing capacity would be seriously impaired. Consequently, this option would require complex and costly structural provisions during the repair period to guarantee the load-bearing capacity. Moreover, from a sustainability point of view, several arguments were raised as this option would result into

the removal of significant amounts of structurally sound concrete.
Lastly, patch repairs combined with cathodic protection was suggested as an interesting option. In view of the widespread occurrence of reinforcement corrosion a cathodic protection system covering the complete soffit surface area is considered to be most effective and efficient. Both an impressed current or a galvanic system are available to achieve sufficient corrosion protection. However, for several reasons an impressed current system is considered less attractive. Such a system requires the use of long cabling, sensors and placement of electronic equipment to frequently control, monitor and adjust its input and output. The asset owner will thus be confronted with planning of these monitoring activities and annual costs. In addition he will be faced with the risk of vandalism of the equipment and the resulting malfunctioning of the protection system which is likely to remain unnoticed for several months. Taking into account these 'undesirable events' inherent to an impressed current system it was anticipated that the application of a galvanic cathodic protection system, combined with patch repairing, would be the most appropriate option.

5 TRIAL APPLICATION OF GALVANIC CATHODIC PROTECTION

The proprietary zinc sheet anode is intended to cover the complete concrete surface. In order to act as an anode the zinc is provided with an ion conductive adhesive which simultaneously acts as an ion conductor, an adhesive, an activator as well as a storage for the non-soluble zinc salts. The protection current is generated through the continuous dissolution of zinc into the ion-conductive adhesive, resulting in the release of negatively charged electrons which are fed to the reinforcement through direct metallic contact between the zinc and the embedded reinforcing steel. This electronic contact can either be made through external wiring or through metallic pins.

In view of the nature of the prevailing exposure conditions, the presence of lightweight concrete and the deep chloride ingress several questions emerged on the long-term effectiveness of such a galvanic system.

With respect to lightweight concrete its electrical resistivity may be significantly different from 'conventional' normal weight concrete and this may affect the magnitude of the current output as well as the spatial distribution of the protection current over the reinforcing steel. If the concrete resistivity would appear to be low then this would result in a reduced overall electrical resistance of the galvanic circuit. Consequently, a higher current output would be generated resulting in a higher zinc consumption rate. Information on the actual zinc consumption rate is required to determine the zinc layer thickness to achieve the required 25 year operational service life of the cathodic protection system.

In view of the deep chloride penetration it was anticipated that not only the first layer of reinforcing steel would need protection current, but also the second layer embedded at greater depth. As the driving voltage of a galvanic system is relatively small (in most situations involving corroding steel the driving voltage is significantly less than 1V), the so-called throwing power in depth as well as in lateral direction will be limited. Thus quantitative information on the throwing power in a lateral direction is considered relevant to determine the borders of the concrete area which should be covered with zinc sheet to achieve sufficient protection of corroding reinforcing steel embedded in neighbouring non-covered concrete areas, see Figure 5. Based on results obtained in 2002 with a similar zinc sheet anode a pronounced attenuation of protection current in the lateral direction was observed and it was concluded that steel embedded at a greater distance than 200mm to the border of the concrete area covered with zinc sheet will not be sufficiently protected against corrosion.

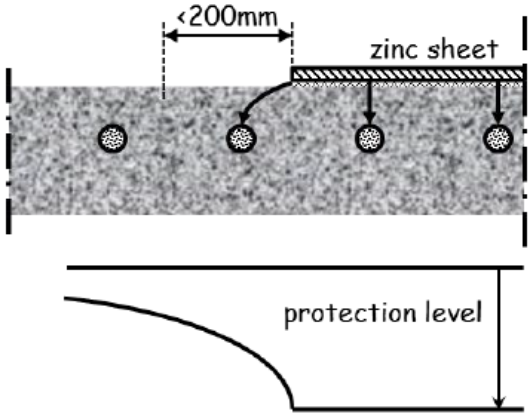

Figure 5. Schematic presentation of the throwing power.

6 CONCLUDING REMARKS

Initially it was envisaged to perform the trial during a period of no more than 6 months, however due to some delays in the tendering stage, the trial eventually lasted nearly 1 year. Based on the results of the trial it was concluded that for this situation encountered at the Neerbossche bridge:

- The throwing power of the zinc sheet in a lateral direction is limited to less than 10cm;
- The second layer of reinforcing steel becomes sufficiently protected;
- The zinc consumption rate is such that the standard layer thickness can be used for a service life of 25 years.

Following these conclusions, the concrete surface area to be covered with zinc sheet was enlarged so as to include neighbouring concrete surfaces which were less suspect of reinforcement corrosion. The decision to enlarge the zinc-covered surface area was considered wise as the throwing power in a lateral direction was very limited. Moreover, the poor accessibility would make it a costly business to apply additional zinc sheet at a later stage.

The zinc consumption rate was such that a standard thickness could be used provided the complete concrete surface area was covered with zinc sheet, i.e. without a spacing between neighbouring strips. This decision was also supported by the fact that covering 50% of the concrete surface with zinc would lead to doubling the zinc thickness so as to achieve a service life of 25 years. Furthermore, using zinc sheet with a smaller width would lead to additional costs for cutting and application on the concrete surface.

Eventually, the zinc strips used for the investigations were left unchanged after the trial, whereas the remaining segments were completely covered with zinc sheet using the standard width and thickness. The measurements on the trial section (2 segments) will continue so as to obtain information on the long term performance of galvanic cathodic protection.

REFERENCES

Boutz, M. 2012a. Investigations on cavities in the cantilever of the Neerbossche bridge – Results of stage 1 Investigations on the soffit of the bridge. Interim Report of SGS INTRON, Sittard (in Dutch).

Boutz, M. 2012b. Investigations on cavities in the cantilever of the Neerbossche bridge – Results of stage 2 Investigation on the top surface of the bridge deck. Interim Report of SGS INTRON, Sittard (in Dutch).

Boutz, M. 2012c. Investigations on cavities in the cantilever of the Neerbossche bridge – Results of stage 3 Investigation on the soffit of the bridge deck. Final Report of SGS INTRON, Sittard (in Dutch).

Broomfield, J. 1997. Corrosion of steel in concrete – Understanding, investigation and repair. London: E&FN Spon.

Christodoulou, C. Tiplady, H., Goodier, C.I. & Austin, S.A. Performance of silane impregnants for the protection of reinforced concrete. In Mike Grantham et al. (eds) *Concrete Solutions 2014. Proceedings of Concrete Solutions, the 5th Int. Conf. on Concrete Repair*, Belfast, 1-3 September 2014. Boca Raton, Fl: CRC Press.

Dai, J.-G., Akira, Y., Wittmann, F.H., Yokota, H. & Zhang, P. 2010. Water repellent surface impregnation for extension of service life of reinforced concrete structures in marine environments: The role of cracks. *Cement & Concrete Composites* 32: 101-109.

Ormellese, M., Berra, M., Bolzoni, F. & Pastore, T. 2006. Corrosion inhibitors for chlorides induced corrosion in reinforced concrete structures. *Cement and Concrete Research* 36: 536-547.Söylev, T.A., McNally, C. & Richardson, M. 2007. Effectiveness of amino alcohol-based surface-applied corrosion inhibitors in chloride-contaminated concrete. *Cement and Concrete Research* 37: 972-977.

Netherlands Normalisation Institute 1984. Regulations for concrete VB 1974/1984 NEN 3880 - Part G Lightweight concrete – Additional clauses. Delft: NNI (in Dutch).

Application of a surface-applied cathodic protection system on a light weight concrete bridge – Part II: Developments in time of the effectiveness by potential decay values and current densities

A.J. van den Hondel MSc
Vogel Cathodic Protection, Zwijndrecht, Netherlands

R.G. Giorgini MSc
CorrPRE, Reeuwijk, Netherlands

J. Gulikers MSc
Rijkswaterstaat-GPO, Utrecht, Netherlands

ABSTRACT: As part of a triptych this paper gives insight in the research and investigations which were undertaken on a post tensioned light-weight concrete box girder bridge in the Netherlands. This project started in the first half of 2013 and measurements are still executed regularly. Due to long-term leakage of a longitudinal joint between two parts of the bridge, chlorides had penetrated into the concrete up to the level of the reinforcement and beyond, causing severe corrosion of the steel, spalling of the concrete cover and eventually causing danger for the shipping underneath the bridge due to falling lumps of concrete. To solve this problem, Galvanic Cathodic Protection (GCP) was applied in 2 stages. Firstly, in 2013, zinc based anode strips were applied on the soffit of 2 post tensioned lightweight bridge segments for the purpose of testing and monitoring. After obtaining good results from the test, in 2014/2015 the remaining 29 bridge segments were repaired and protected with the same GCP system as well.

This paper reviews subsequent potential decay measurements, which have provided much more information on GCP performance and throwing power. The results of anode performance at different locations and depths are reviewed. Repair mortars and the moisture content of the concrete have also shown a major influence on the behavior of the installed GCP system.

Figure 1. The Neerbossche Bridge over the Maas-Waal canal.

1 INTRODUCTION

1.1 *The object*

The object concerns the Neerbossche Bridge which spans the Maas-Waal canal at Nijmegen, The Netherlands (Figure 1). The bridge is a post tensioned double box girder bridge from 1982, of which the structure above the canal is constructed with light-weight concrete (1650 kg/m^3). The in-situ cast concrete segments have a length of about 3.4 meters. For each box girder, the part of the bridge located between the piers comprises 33 segments of which the 2 segments above the piers are constructed with conventional normal weight concrete. So each box girder is comprised of 31 light-weight concrete segments above the canal. The soffit of the light-weight concrete sections of the southern box girder showed serious damage and consequently maintenance was required in the short term in view of structural safety as well as possible danger for the shipping underneath the bridge due to falling lumps of concrete.

1.2 *The project*

The damage in the bridge was extensively investigated and reported in a preliminary phase and it was concluded that the damage was limited to the concrete surface at the soffit of the northern cantilever of the span of the southern bridge (Figure 2). Due to long-term leakage in the longitudinal joint between the northern and southern bridge, chlorides originating from the frequent application of de-icing salt during winter periods had penetrated into the concrete up to the level of the reinforcement and beyond. As a consequence, the mild steel reinforcement had started to corrode which eventually resulted in the development of significant tensile stresses in the concrete, leading to cracks, delaminations and spalling at multiple locations. The corrosion induced damage amounted to approximately 44 m^2, which was about 22% of the total surface of the soffit. At other locations, the likelihood of corrosion was demonstrated by corrosion potential measurements which showed values down to -450 mV (Cu/CuSO$_4$) and -350 mV (Ag/AgCl; see Figure 3).

As a long-term solution to this problem, cathodic protection (CP) was considered to present a viable and economical option. As the structure was post tensioned, Galvanic Cathodic Protection (GCP) was in favor to be applied in order to avoid the risk of hydrogen embrittlement in the high quality steel tendons. In the summer of 2013 the steel reinforcement in 2 bridge segments was protected with zinc based strip anodes, for testing purposes applied in small size foils which could be connected to the reinforcing steel on and off separately. Also a large number of reference electrodes (titanium decay probes, referred to as RE's) were embedded in the concrete of

Figure 2. Location of the damaged cantilever (southern bridge).

these 2 segments in order to monitor the effectiveness of the CP system, not only within the protected area but also outside the protected area.

With these 'remote' RE's the so-called throwing power of this CP system could be established. For the same reason RE's were installed at different depths in the concrete cover as well as in repaired areas in order to study the corrosion behavior of the steel in these areas due to the action of the CP system.

In view of the good results that were obtained in this test and the suitability of this GCP system was proven, the full scale project on the remaining 29 bridge segments was executed in the winter of 2014/2015.

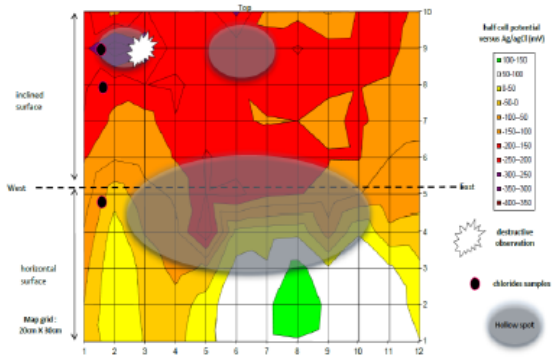

Figure 3. Corrosion potential measurements at the cantilever in the southern bridge. The grey areas denote hollow spots and the white flash a destructive investigation point.

1.3 *Scope of the paper*

This paper is part II of a triptych. Part I gives detailed information on the preliminary phase and also on the process of selecting the preferred repair strategy and finally on the results from the test in 2013.

This part II will focus on the highlights of the full scale project in 2014/2015 and will provide results from the still ongoing research and investigation on the effectiveness of the GCP system over time, by measuring potential decay values and current densities.

2 THE APPLICATION OF THE GCP SYSTEM

2.1 *Accessibility of the soffits*

The canal underneath the bridge and the location of the cantilever in between the two box girders, at a height of approximately 10 meters above the water level, resulted in poor accessibility. In the past, a vessel with a scaffolding was used for the investigations on this part of the bridge, but due to the busy shipping on the canal and the instability of this kind of construction at a height of 10 meters it was not suitable for the extensive project. A new way for accessibility, developed in the USA, used cables across the canal to create a suspension bridge (Figure 4& 5). This solution resulted in a good and safe access to the soffit, with no hindrance to the shipping and the possibility to create a closed environment above the water (preventing pollution of the water surface and enabling to work during the winter period).

Figure 4. The access to the soffit at the damaged cantilever.

Figure 5. The workspace created underneath the bridge.

2.2 *Concrete repair*

The concrete was repaired in accordance with the code based international standards (ISO-EN12696) regarding the surface pretreatment, instead of a full traditional repair with the removal of all chloride-contaminated concrete. Therefore, only the spalled and delaminated concrete parts were removed, the corroded steel bars were sandblasted up to a level of St2 after which a mineral-based mortar was applied to achieve a smooth surface.

The mortar had to be chosen carefully because the light-weight concrete had special features regarding water absorption, aggregates and tensile strength. A good bonding of the repair mortar on to the light-weight concrete had to be achieved, thus the shrinkage of the mortar, the initial absorption of water from the fresh mortar into the old concrete and the water and cement content of the repair mortar had to be adjusted for the two materials. At the same time the mortar had to be suitable for the application of CP, mainly with regard to the electrical resistivity of the mortar. In accordance with the code based CP standards the resistivity of the mortar should not be less than 50% of the resistivity of the original light-weight concrete and should not exceed 200% of this value. Depending on the location, mainly with regard to the moisture conditions, the resistivity measured with a Wenner probe varied between 100 to 500 Ωm in the areas adjacent to the leaking joint and up to 2500 Ωm at the dryer side of the box girder.

Because of the importance of this part of the maintenance, the type of mortar as well as the method of applying the mortar to the surface, was part of the test in 2013 and resulted in the application of shotcrete using a light-weight mortar with a high cement content and no additives (Figure 6). Shotcreting resulted in less shrinkage and better bonding to the original surface (1.3 – 1.7 N/mm^2). The mortar (Grouttech NSM Multirep) demonstrated resistivity values ranging from 110 to 160 Ωm measured at 100% RH and 7100 to 7500 Ωm at 35% RH and therefore met the requirements.

Figure 6. Repair of the damaged locations with shotcrete.

Before the mortar was applied, the surface at the repair location was treated by drilling in dowels (16 Hilti M8-100 per m^2). This is common practice in the application of shotcrete at pending surfaces in order to withstand the stresses due to shrinkage of the fresh mortar. Also, the light-weight concrete surface was, prior to the spraying of shotcrete, pre-moistened several times to prevent water being adsorbed from the applied fresh mortar. Finally, the shotcrete was applied in 2 successive layers, result-

ing in a total thickness between 20 and 50 mm. The first layer was sprayed with a thickness of 10 mm in order to achieve a good adhesion with the lightweight concrete substrate. Subsequently, after 2 hours, the second layer was applied to the appropriate thickness. Thereupon, the surface was finished in profile and protected against drying out with polythene sheets for 7 days.

2.3 *Cathodic Protection*

After having repaired the concrete, the steel reinforcement was protected with a surface mounted anode, i.e. a Zinc Layer Anode (ZLA; CorrPRE). This anode is applied as a foil on the surface and consists of a 250 µm thick zinc sheet provided with a 750 µm thick ion-conductive adhesive. The adhesive is designed to adhere the zinc strip onto the concrete surface, while simultaneously acting as a zinc activator and conducting electricity.

Based on corrosion potential measurements and the test results on the 2 bridge segments performed in 2013 it was concluded that the complete surface of the soffit should be covered with the zinc anodes (Figure 7). As there was no economic benefit in the application of ZLA in strips with a certain spacing, in order to save material costs, the complete concrete surface was covered with zinc strips using the standard width of 25 cm. The `protection period´ of the ZLA (i.e. material consumption over time) in relation to the cost for accessibility at the moment of an earlier replacement of anode material, made it clear that the application of extra ZLA would have a beneficial impact on the lifetime costs of the CP system.

Figure 7. Application of the zinc anode in strips.

The 25 cm zinc strips were electrically connected by overlapping each strip slightly and shooting steel nails at a distance of one meter into the overlap (Figure 8). Connections to the steel reinforcement (the cathode) were made at 2 separate locations at each bridge segment. Finally the complete zinc surface, including the edges, was covered with a 2 mm thick layer of BASF 6100FX (a waterproof cement based coating) in order to prevent the zinc from direct contact with moisture due to condensation and the resulting atmospheric corrosion.

Figure 8. Connections at the overlaps of the zinc strips.

3 DEVELOPMENTS IN TIME OF THE EFFECTIVENESS OF THE GCP SYSTEM

3.1 *The test segments*

The original test provisions from 2013 on the 2 segments (Figure 9), with a large amount of RE's and the narrow zinc strips (with a width of 83 mm), were kept unchanged, as much as possible, during the full scale project in 2014/2015 in order to be able to continue the monitoring of the GCP system and to start research of the long-term effects of this type of GCP systems with a surface mounted anode. Since 2013 depolarisation measurements of the CP system in different seasons have been carried out, using all the RE's in and remote from the protected area, as well as in depth. The amount of protection current being generated by each zinc strip was measured and monitored in order to predict the service life of the (sacrificial) anodes. Also other system parameters, such as the resistance in all the components, were monitored. These measurements were carried out during 2.5 years and show interesting results, expanding the knowledge on GCP and the long-term effects on potential decay values, (protective) current densities and the throwing power of galvanic anodes, as well as the influence of repair mortars and the moisture content of the concrete on the behavior of installed GCP systems.

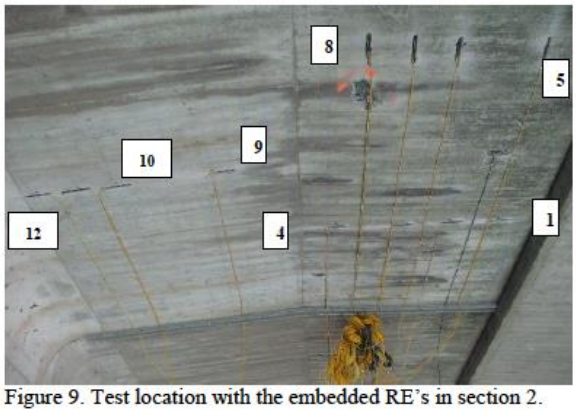

Figure 9. Test location with the embedded RE's in section 2.

3.2 *Data and properties of the test segments*

Two bridge segments were selected in 2013:

1. Segment 2 (of 33) with 4% of concrete damage, a concrete cover between 29 mm and 45 mm (μ = 37 mm) and corrosion potential measurements with values from 0 mV down to -270 mV ($Cu/CuSO_4$)
2. Segment 3 with 33% of concrete damage, a concrete cover between 25 mm and 46 mm (μ = 38 mm) and corrosion potential measurements with values from -30 mV to -350 mV (at the location of the damage)

The reinforcement of the soffit was placed in 2 layers, crosswise, with rebars of Ø12 mm and Ø16 mm in diameter

The carbonation depth as measured in the soffit varied between 2 mm to 11 mm, however high chloride contents were measured, up to 3% on cement weight and up to depths of over 50 mm.

The CP system at the test segments was applied on the horizontal part of the cantilever and the adjacent 50 cm of the inclined segment (thus over a total width of approximately 2 meters). Each test segment was in this way covered with approximately 6,2 m^2 of ZLA (Figure 10).

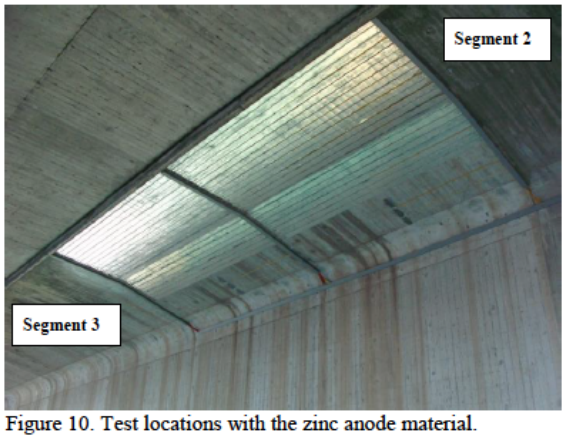

Figure 10. Test locations with the zinc anode material.

3.3 *Effectiveness of the installed GCP system*

The measurements were carried out using the titanium decay probes (RE's), embedded in the concrete of the first 2 segments, in and remote from the protected area.

From the start in 2013, the measurements showed that the applied GCP system was effective. The depolarisation (potential decay) values met the code based CP criteria (ISO-EN12696) i.e. a minimum of 100 mV depolarisation after 24 hours or 150 mV after complete depolarisation (Figure 11 and 12), with the exception of 1 RE in segment 3.

Section 2

Date	28-8-2013	22-11-2013		28-1-2014	4-12-2014	20-3-2015	16-10-2015
Session	1e	3e		4e	7e	8e	9e
	Depolarization						
	(-mV)	(-mV)	(-mV)	(-mV)	(-mV)	(-mV)	(-mV)
RE 1	240	255	461	376	157	263	300
RE 2	387	344	387	452	188	240	304
RE 3	217	211	241	214	83	109	101
RE 4	231	217	225	226	101	155	123
RE 5	146	151	160	131	61	87	95
RE 6	157	158	165	173	77	130	121
RE 7	187	188	237	234	108	139	141
RE 8	224	229	320	271	116	190	173
RE 9	270	334	481	324	226	289	184
RE 10	101	104	163	148	72	104	2
RE 11	64	69	90	90	49	60	31
RE 12	47	48	74	69	37	45	13
Hours of depol	24	24	168	144	23	74	240
Threshold value	100 mV	100 mV	150 mV	150 mV	100 mV	150 mV	150 mV

First layer of reinforcement
Second layer of reinforcement
Most negative potential
Remote from CP area: 20 / 40 / 60 cm

Section 3

Date	28-8-2013	22-11-2013		28-1-2014	4-12-2014	20-3-2015	16-10-2015
Session	1e	3e		4e	5e	7e	8e	9e
	Depolarization							
	(-mV)	(-mV)	(-mV)	(-mV)	(-mV)	(-mV)	(-mV)	(-mV)
RE 1	134	156	152	164	152	62	77	210	185
RE 2	154	177	184	202	210	104	91	268	196
RE 3	112	133	120	232	231	135	112	293	240
RE 4	58	64	57	89	149	77	101	320	192
RE 5	130	147	122	137	141	60	75	313	221
RE 6	74	85	89	114	144	66	33	310	188
RE 7	58	65	67	77	89	53	50	247	211
RE 8	51	58	53	66	76	53	59	193	216
RE 9	51	57	52	73	74	25	36	202	221
RE 10	31	39	36	46	70	37	38	209	215
RE 11	285	333	294	309	533	307	192	363	180
RE 12	87	102	101	150	138	86	82	81	33
RE 13	56	65	57	85	84	57	54	58	21
RE 14	25	49	29	72	60	41	40	26	-1
Hours of depol	24	79	24	168	144	26	28	74	240
Threshold value	100 mV	150 mV	100 mV	150 mV	150 mV	100 mV	100 mV	150 mV	150 mV

zinc anode material
First layer of reinforcement
Second layer of reinforcement; partly in repair locations
In repair locations
Most negative potential
Remote from CP area: 20 / 40 / 60 cm

Figures 11 & 12. Depolarisation values of segments 2 and 3.

Furthermore it was found, from the RE's placed at different depths in the concrete cover, that in segment 2 the second layer of reinforcement was protected as well. However, in segment 3, only 1 of the 4 RE's met the code based CP criteria, although it should be noted that 2 of the RE's which did not comply with these criteria were placed in repaired locations (RE7 & RE8). In general, the depolarisation values of the second layer were less compared to the ones located in the first layer of reinforcement. In the first 4 months after installation of the CP system, as an average, 70% and 66% of the potential decay values of the first layer were measured at the second layer of reinforcement in segments 2 and 3, respectively.

The best results in segment 3 were clearly obtained for the reinforcement showing the most negative natural potentials prior to installation of the CP system (RE11). In segment 2, the depolarisation values of the similar reference electrode (RE9) were also more than satisfactory with an average of 302 mV in the first 4 months after installation.

The measurements also showed that the CP system was not only effective in the protected area but also at a limited distance from the protected area, at least up to 20 cm.

Finally, RE's placed in repaired areas (segment 3; RE 7-10) showed less depolarisation than similar RE's in non-repaired locations. The depolarisation values did not meet the code based criteria.

3.4 *Developments in time of the potential decay values*

The measured values of the depolarisation in the protected area decreased over time (Figures 13 and 14). At the start in 2013 the measurements showed higher values indicating that the applied GCP system complied with the code based ISO-EN12696 criteria at almost all locations where RE's are installed, resulting in sufficient protection of the reinforcement. More than 2 years later (in October 2015) only 3 out of 5 RE's (60%) at the first layer of reinforcement in segment 2 still met the code based protection criteria (compared to 100% compliance in 2013). Drying out of the concrete and polarisation of the steel are considered to be the explanation for this observation.

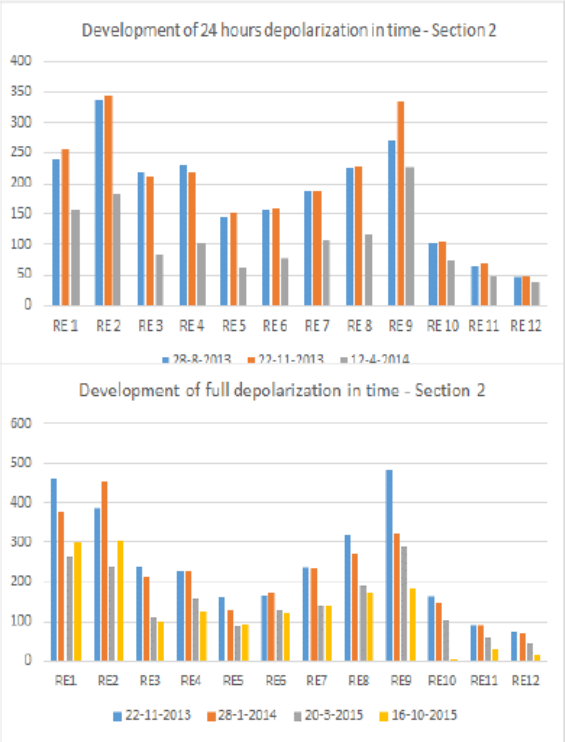

Figures 13 & 14. Development of depolarisation values in time of segment 2.

At segment 3, a part of the zinc anode, as well as some RE's, were replaced during the full scale project in December 2014 due partly to repair mortar disbondment during the test phase. As a consequence, the last measurements with the original anode material dated from December 2014 showing similar results as obtained for segment 2. In segment 3, 17 months after installation, also 3 out of 5 RE's (60%) in the first reinforcement layer met the code based protection criteria (compared to 80% compliance in 2013). The best result in this segment was still coming from the reinforcement with the most negative natural potentials prior to CP installation (RE11).

At the same time, from the RE's placed at the second layer of reinforcement only 1 out of 4 RE's (25%) in segment 2 and none of them in segment 3 (0%) met the code based criteria (compared to 100% and 50% compliance in 2013 respectively).

After replacing a part of the zinc anode and repairing the disbonded areas with the selected type of shotcrete at segment 3 (December 2014), the system reacted immediately and showed good results again. The GCP system (with partly new zinc anode material) met the code based criteria again, indicating sufficient protection of the reinforcement at all locations where RE's are installed i.e. at both the first and second reinforcement layer and in the repaired areas. Moisturizing of the concrete and the new installed anode material can be the explanation for this observation.

At the areas located more remote from the anode, i.e. adjacent to the protected surface, similar observations were found. At the start in 2013 the protected area stretched out at least up to 20 cm adjacent to the anode material. More than 2 years later this positive side effect was no longer measured with the RE's at a distance of 20 cm from the anode material. Drying out of the concrete is considered to be the explanation for this observation.

Finally, the RE's placed in repaired areas (segment 3; RE 7-10) showed, after having replaced the zinc anode and the disbonded areas (December 2014), sufficient depolarisation at all locations. The most probable explanation for the negative outcome of the potential decay values at these RE's during the first 17 months lies in disbondment of the repair mortar.

3.5 *Developments in time of the current density*

The current output readings were carried out for each separate zinc foil (22 strips per segment with a width of 83 mm and a total zinc surface of 0.28 m^2 for each strip) at 3 points in time. The total current output was measured as well for the complete anode system per segment (with a total zinc surface of 6,2 m^2).

The measured current outputs strongly decreased over time (Figures 15 and 16). At the start in 2013 the total current output amounts to 28.6 mA (equal to 4.6 mA/m^2_{anode} and approximately 7.7 mA/m^2_{steel}) and 24.8 mA (equal to 4.0 mA/m^2_{anode} and approximately 6.7 mA/m^2_{steel}) for segment 2 and 3, respectively. After 14 months it was reduced to 5.4 mA (equal to 0.9 mA/m^2_{anode} and approximately 1.5 mA/m^2_{steel}; a reduction of 81%) and 6.8 mA (1,1 mA/m^2_{anode} and approximately 1.8 mA/m^2_{steel}; a reduction of 73%).

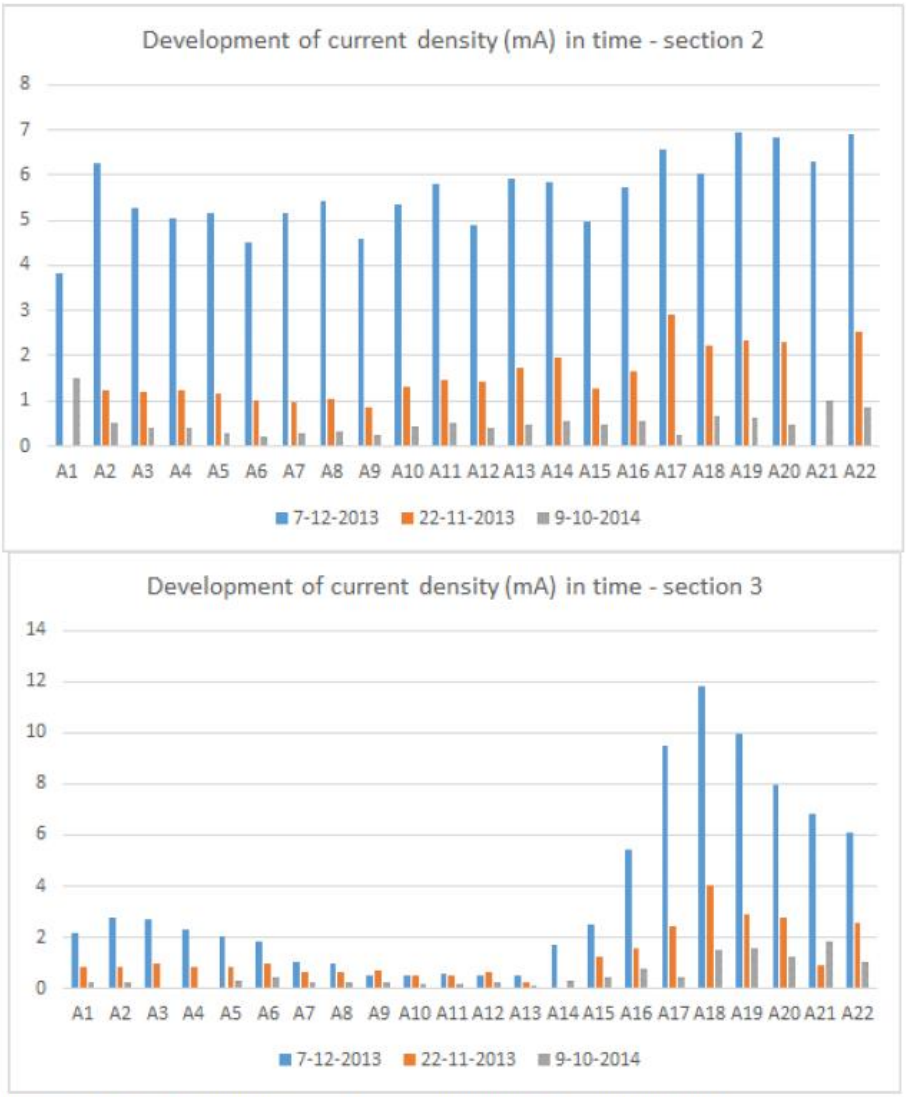

Figures 15 & 16. Development of the total current output in time for segments 2 and 3.

The current outputs for each separate zinc foil (22 strips per segment) varied strongly in segment 3. The parts of segment 3 with small patched areas, between zinc strips A5 to A8 and A14 to A16, and the parts of this segment with larger patched areas, between zinc trips A9 to A13 (Figures 17 and 18), showed a lower current output compared to the non-patched areas. Specifically zinc strips A17 to A22 showed much higher current outputs.

The zinc strips applied in segment 2, which has less patched areas, showed more equally distributed current outputs.

Patched areas were shown to have a major influence on the current output of the zinc strips. The observed decrease in the current outputs could be caused by the disbondment of the repair mortar in the test phase, as mentioned before.

To compare the current output of each zinc strip vs the potential reading of respective RE's is complicated due to the fact that the RE is affected by the current output of all neighboring zinc strips.

Figure 17. Repair locations and RE's in segment 3.

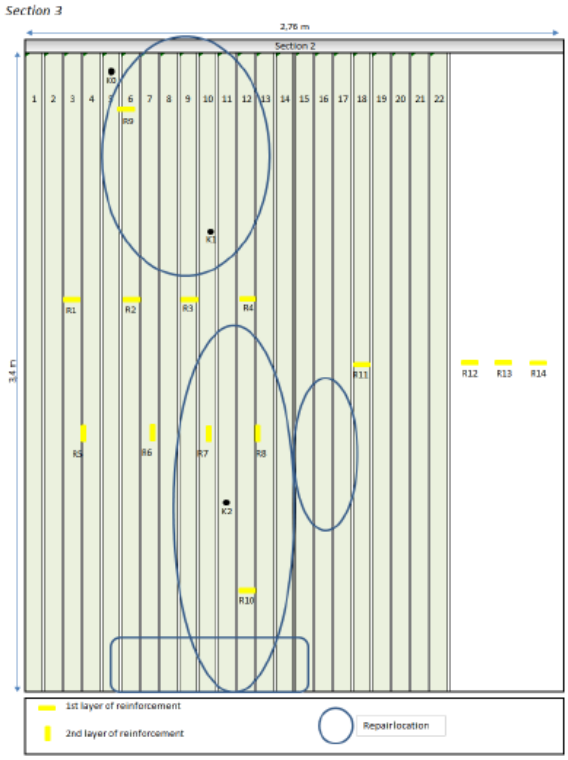

Figure 18. Anode strips, RE's and repair locations in segment 3.

3.6 *Developments of the concrete resistance in time*

The measurements of the concrete resistance were carried out by measuring the resistance between each individual RE and the reinforcement.

The measured values of the concrete resistance on these specific locations increased strongly over time. At the start in 2013 the measured resistances in segment 2 varied between 1 to 9 kΩ, in segment 3 in the patched areas between 0.4 to 0.7 kΩ and between 1 to 6 kΩ in non-patched areas. After 14 months, it increased substantially and the resistances varied at that moment from 7 to 212 kΩ in segment 2 and in segment 3 from 2 to 5 kΩ in patched areas and from 4 to 130 kΩ in non-patched areas.

4 CONCLUSIONS

4.1 *General*

Since 2013 potential decay values, current outputs and resistances were measured during a period of 2.5 years on 2 selected bridge segments in which a large amount of RE's were installed and on the narrow surface zinc strip anodes. These measurements showed interesting results on the effectiveness of the installed GCP system with surface-mounted zinc strip anodes (ZLA), on the development of the long term potential decay values and (protection) current outputs, and on the throwing power of galvanic anodes. The type and location of repair mortars used and the moisture content of the concrete were identified to have a major influence on the behavior of the installed GCP system.

Monitoring of the installed CP system will continue and will be further reported in the future.

4.2 *Effectiveness of the installed GCP system*

From startup (2013) the measurement results have demonstrated that the applied GCP system resulted in an effective solution. The depolarisation values complied with the code based protection criteria (ISO-EN12696) at almost all of the locations where RE's were installed.

The second reinforcement layer was protected as well (in non-patched areas), however with substantially less potential decay values compared to the first reinforcement layer.

The CP system was not only effective in the anode covered area but also more remote from the covered area, at least up to 20 cm.

RE's located in patched areas showed less depolarisation compared to similar RE's in non-patched areas. The corresponding depolarisation values did not meet the code based protection criteria for CP but this was most probably caused by partial disbondment of the repair mortars during the test phase.

4.3 *Potential decay values over time*

Depolarisation values gradually decreased over time and part of the installed RE's after 1.5-2.5 years showed values which did not comply with the code based protection criteria anymore, predominantly the readings from RE's installed at the depth of the second reinforcement layer. Drying out of the concrete and polarisation of the steel are considered to be the explanation for this observation.

In December 2014, i.e. during the full scale project, some zinc strip anodes needed to be replaced because of the disbondment of repair mortar during the test phase. After replacing the zinc strips and repairing the disbonded areas, the system reacted immediately and showed good results again. Moisturizing of the concrete and the new installed anode material are considered to be the explanation for this observation.

The effectiveness of the CP system to protect steel located at more distance from the protected area decreased over time as well. After more than 2 years this positive side-effect was no longer measured with the RE's placed at a distance of 20 cm from the anode material. Drying out of the concrete is considered to be the explanation for this observation.

4.4 *Current outputs over time*

The current outputs decreased strongly over time. At the start in 2013 the total current output was approximately 4 - 5 mA/m^2_{anode} (equal to 6.5 - 8 mA/m^2_{steel}) which was reduced in 14 months to approximately 1 mA/m^2_{anode} (equal to 1,5 - 2 mA/m^2_{steel})

The current outputs at patched areas were less than at non-patched areas. At spots where no or just minor patched areas were present, the current outputs were more equally distributed.

Patched areas were shown to have a major influence on the current output of the zinc strips. However, this could have been caused by the disbondment of the repair mortar in the test phase and will be investigated in the coming year.

5 REFERENCES

ISO-EN12696:2012, *Cathodic protection of steel in concrete*. Geneva: ISO.

CUR Aanbeveling 45, 1996. *Cathodic Protection of reinforcement in concrete constructions* (in Dutch, Kathodische bescherming van wapening in betonconstructies). Gouda: CUR.

Van Den Hondel, A.J., 2015. *Execution of concrete repairs with the use of galvanic CP – Neerbosschebrug Nijmegen* (in Dutch, Uitvoering van betonherstel met een galvanisch KB-systeem - Neerbosschebrug Nijmegen). Utrecht: RWS.

Assessment of the throwing power generated by a surface applied galvanic cathodic protection system on a light weight concrete bridge deck soffit.

R. Giorgini
CorrPRE Engineering BV, Reeuwijk, Netherlands

Hans van den Hondel
Vogel Cathodic Protection BV, Netherlands

Joost Gulikers
Dutch Ministry of Infrastructure and the Environment, Netherlands

ABSTRACT : As part of a triptych this paper will give insight in the research project which was carried out on a prestressed lightweight concrete bridge located in the Netherlands. This project started in the first half of 2013 and measurements are still ongoing on a regular basis.

Years of leakage at the longitudinal joint in between both bridge decks allowed chlorides to penetrate into the bridge deck soffit causing severe corrosion of the mild steel reinforcement eventually resulting in significant cracking and spalling of the concrete cover. As an economic remediation solution it was recommended to apply a cathodic protection (CP) system, preferably a galvanic CP system avoiding hydrogen embrittlement in the prestressed tendons.

Generally, it is assumed that only the reinforcing steel located beneath the concrete surface provided with surface applied zinc sacrificial foil will be protected. The objective of these on-site investigations is to have a better indication of the so-called throwing power by measuring the depolarization behavior at 3 different distances from the border of the zinc foil. Since 2013 potential decay values, current output and resistance of each separate zinc layer were monitored of the initial two zones in order to predict the service life of the zinc sacrificial system. The measurement results obtained so far indicate a major influence of the repair mortars used and moisture content of the concrete on the behaviour of the installed GCP system.

1 INTRODUCTION

This paper presents the set-up and the findings of a research project which was carried out on a prestressed lightweight concrete (1650 kg/m^3) bridge "Neerbosschebrug" located in the Netherlands. The investigations started in the first half of 2013 and measurements are still continuing on a regular basis.

Years of leakage at the longitudinal joint in between two parallel bridge decks allowed chlorides originating from the application of de-icing salt in winter periods to penetrate into the bridge deck soffit initiating corrosion of the mild steel reinforcement which eventually resulted into significant cracking and spalling of the concrete cover. As an economic remediation solution it was recommended to apply a cathodic protection (CP) system preferably a surface-applied galvanic CP system as this would pose no risk of hydrogen embrittlement in the prestressed tendons.

Generally, it is assumed that only the reinforcing steel located directly beneath the concrete surface provided with surface-applied zinc sacrificial foil will be protected. The objective of these on-site investigations is to have a better indication of the so-called "throwing power" by measuring the depolarization behavior at 3 different distances from the border of the zinc foil. In view of this, since 2013, potential decay, current output and resistance of 22 zinc strips were monitored in two bridge sections, in order to obtain a more reliable estimate of the effective service life of the zinc sacrificial system. The results achieved so far indicate a major influence of the repair mortars used and moisture content of the concrete on the behaviour of the installed GCP system.

2 EXPERIMENTAL PROCEDURE

The ZLA "zinc layer anode" system was applied in long strips over a length of 3.4m (bridge section length) covering a width of 2m divided over 2 bridge sections (section 2 and 3 of the northern part of the bridge). The zinc anode was applied on the concrete surface by using 22 strips of 8cm width with a spacing of 1cm between the strips.

Prior to application of the zinc strips the spalled and cracked areas of both sections were repaired. In section 2 approximately 2% of the total surface area was repaired and in section 3 a total of 33%. Two types of sprayed concrete mortars were used :

- Weber.tec SBN 170
- Grouttech NSM Multirep

At the soffit in both sections, Ø12mm and Ø16mm bars were used with a concrete cover varying between 25mm and 46mm. For section 2, the average cover depth amounted to 37mm and for section 3, an average of 38mm was detected. According to the design drawings, the distance between the first and second reinforcement mat amounts to 50mm.

The following listing presents a summary with technical details of the test area of each section.

Figure 1. Spalled area of section 3.

Section 2

- 2 cathode contacts and on/off K_0-switch for monitoring purposes ;
- 22 zinc layer anode strips, width 8 cm, with a distance of 1cm between neighbouring strips, anode surface area appr. 7 m^2 per section.
- each zinc anode strip is provided with an external electric contact.
- 8 Ti-decay probes (RE) :
  - 4 RE's : R1 to R4 located at the depth of the first reinforcement layer,
  - 4 RE's : R5 to R8 located at the depth of the second reinforcement layer,
  - No RE's installed in the patch area.
- 4 Ti-decay probe RE's lined up partly in and beyond the anode area in the first rebar layer in a zone with most negative natural potentials, non patched area :
  - R9 within the anode area,
  - R10 at 20cm distance from the anode area,
  - R11 at 40cm distance from the anode area,
  - R12 at 60cm from the anode area.

Section 3

- 2 cathode contacts and on/off K_0-switch for monitoring purposes ;
- 22 zinc layer anode strips, width 8 cm, with a distance of 1cm between the each strip, anode surface area appr. 7 m^2 per section.
- 22 external anode contacts.
- 8 Ti-decay probes (RE) :
  - 4 RE's : R1 to R4 embedded at the depth of the first reinforcement layer,
  - 4 RE's : R5 to R8 located at the level of the second reinforcement layer,
  - 2 RE's : R9 and R10 in the patched area.
- 4 Ti-decay probe RE's lined up partly in and beyond the anode area in the first rebar layer in a zone showing the most negative natural potentials, non patched area :
  - R11 within the anode area,
  - R12 at 20cm distance from the anode area,
  - R13 at 40cm distance from the anode area,
  - R14 at 60cm from the anode area.

Figure 2. Zinc strips applied on section 2 and 3.

All other necessary parameters of the test area were checked and approved, comprising :

- reinforcement steel continuity,
- resistance of each anode strip,
- anode and cathode connections,
- and the resistances and potentials of the reference cells,

3 RESULTS

On July 12, 2013 shortly after the start-up of the system, the resistances, the current outputs and potential decay values were measured. The readings are shown in Tables 1 to 4. The initial current output for section 2 was 28 mA whereas for section 3 an output of 25 mA was measured. These outputs correspond to approximately 3.5-4 mA/m^2 concrete surface area.

The readings of the decay probes R5 to R8 located in section 2 and 3 at the depth of the 2nd rebar layer (approximately 8-9cm) as given in Table 3 and 4, indicate a good response of the steel on the current output although the surface area was repaired. During approximately 4 months, the response of the decay probes R5 to R8 located in section 2 was relatively poor (between 33-59 mV depolarisation) although they recovered well after that period.

Three Ti-decay probes in section 2, R10 at 20cm, R11 at 40cm, and R12 at 60cm distance from the anode area and 3 Ti-decay probes in section 3, R12 at 20cm, R13 at 40cm, and R13 at 60cm distance from the anode area, show limited response which was not sufficient for full protection according to the protection criteria in the codes. During the first year decay probes R10 in section 2 and R13 in section 3 both at 20cm distance from the anode showed good response in accordance with the code-based criteria but this gradually reduced in the course of the second year.

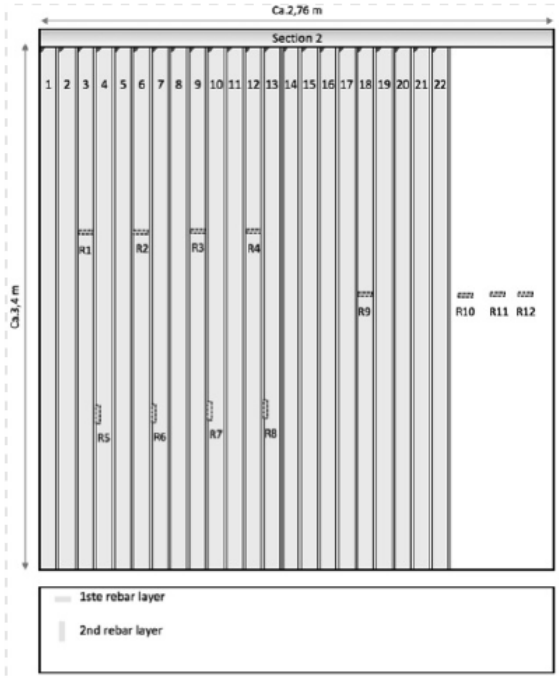

Figure 3. Section 2 : sketch of the anode configuration and decay probes

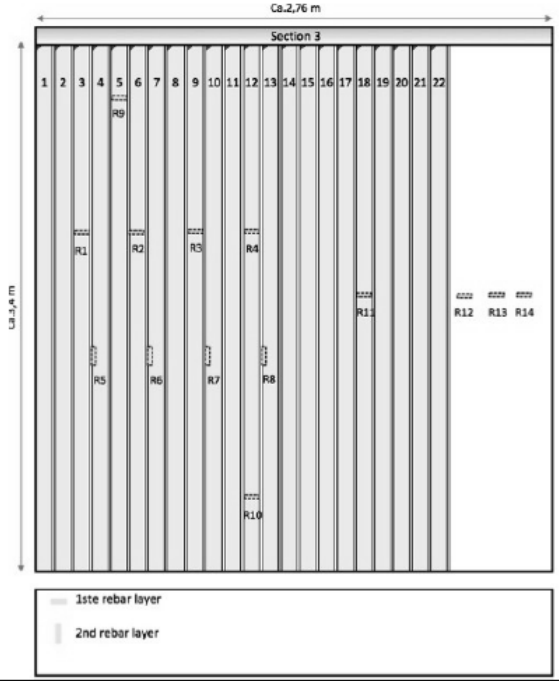

Figure 4. Section 3 : sketch of the anode configuration and decay probes.

Table 1, Section 2, Resistances, Potentials and current outputs of each anode strip.

SECTION 2

Strip nr.	Al	A2	A3	A4	A5	A6	A7	A8	A9	A10	A11	A12	A13	A14	A15	Al6	A17	A18	A19	A20	A21	A22
Ohm	217	112	129	136	137	152	128	121	148	126	116	138	112	121	139	122	108	113	105	57	113	105
Potential my	###	985	960	943	955	923	916	937	910	909	918	896	900	916	895	904	922	904	930	930	927	953
Current mA	3.8	6.3	5.3	5.1	5.1	4.5	5.2	5.4	4.6	5.3	5.8	4.9	5.9	5.9	5	5.7	6.6	6	7	6.8	6.3	6.9

Table 2, Section 3, Resistances, Potentials and current outputs of each anode strip

SECTION 3

Strip nr.	Al	A2	A3	A4	A5	A6	A7	AS	AS	A10	All	Al2	A13	A14	A15	A16	A17	A18	A19	A20	A21	A22
Ohm	277	216	226	265	297	321	568	546	11.76	1115	960	1368	812	606	229	109	54	43	41.	75	97	108
Potential mV	956	920	921	904	890	881	831.	752	763	769	744	832	696	781	843	774	805	838	808	821	880	860
Current mA	2.2	2.8	2.7	2.3	2.0	1.8	1.1	1.0	0.5	0.5	0.6	0.5	0.5	1.7	2.5	5.5	9.5	11.8	10.0	8.0	6.8	6.1

Table 3, Section 2, potential decay values

SECTION 2										
28/8/13	27/9/13	22/11/13	28/1/14	28/3/14	10/9/14	4/12/14	2/3/15	16/10/15		
depolarisation										
24hr mV	3hr mV	24hr mV	3hr mV	144hr mV	26hr mV	23hr mV	74hr mV	240hr mV	RE	
240	151	461	376	148	132	157	263	300	R1	1st layer
337	203	387	452	123	138	183	240	304	R2	
217	108	241	214	64	65	83	109	101	R3	
231	134	225	226	75	79	101	155	123	R4	
146	76	160	131	42	55	61	87	95	R5	2nd Layer
157	92	165	173	66	68	77	130	121	R6	
187	162	237	234	72	78	108	139	141	R7	
224	141	320	271	92	111	116	190	173	R8	
270	314	481	324	182	166	226	289	184	R9	1st Layer
101	64	163	148	48	60	72	104	2	R10	
64	29	90	90	19	34	49	60	31	R11	
47	18	74	69	11	22	37	45	13	R12	

Table 4, Section 3, potential decay values

SECTION 3										
31/8/13	31/8/13	27/9/13	29/11/13	28/1/14	3/2/14	10/9/14	4/12/14	23/3/15	16/10/15	
depolarisation										
24hr mV	**79ht** mV	**3hr** my	**24hr** mV	**3hr** mV	**144hr** mV	**26hr** mV	**23hr** mV	**74hr** mV	**240hr** mV	**RE**
134	155	99	177	82	152	62	77	210	185	**R1**	1st layer
154	177	128	210	131	219	104	91	268	196	R2	
112	133	73	134	117	231	135	112	293	240	R3	
58	64	31	69	103	149	77	101	320	192	R4	
130	147	105	131	95	141	60	75	313	221	R5	2nd Layer
74	85	60	85	87	144	66	33	310	188	R6	
58	65	42	68	50	89	53	56	247	211	R7	
51	58	36	52	44	76	53	59	193	216	R8	
51	57	35	51	39	74	25	36	202	221	R9	1st Layer
31	39	23	39	45	70	37	38	209	213	R10	
285	333	195	298	453	533	307	192	363	180	R11	
87	102	75	103	87	138	86	82	*81*	33	**R12**	outside the anode area
56	65	38	57	40	84	57	54	38	21	**R13**	
25	49	22	31	25	60	41	40	26	-1	**R14**	

4 DISCUSSION

According to the commonly applied international codes for cathodic protection, e.g. ISO12696, reinforcement steel is considered to be sufficiently protected against corrosion when a potential decay values of at least 100 mV from "instant off" is achieved over a maximum period of 24 hours or when a continuous potential decay over an extended period beyond 24 hours of at least 150 mV from "instant off" .

Current measurements seem to have minor significance for the evaluation of protection of cathodic protection systems because the potential shift depends on the polarisation resistance of the reinforcement steel. It should be noted that the current densities mentioned in these codes are only meant to be used for design purposes and not as protection criteria.

The potential decay values in the tables demonstrate that most reference electrodes located near the first steel mesh layer respond well on the current output of each anode strip in both sections 2 and 3. A similar conclusion applies to the reference electrodes R5, R6, R7 and R8 located at a deeper level near the second steel reinforcement layer, taking into account the potential decay time in hours and seasonal effects which can be seen from the potential variations.

Readings of the reference electrodes R12, R13 and R14 located in section 3 show a gradual decrease of the potential response for a given current output of the anode which reflects the attenuation of the electric field in the concrete. The distance of the reference electrodes R12, R13, and R14 are 20cm, 40cm and 60cm, respectively, from the outermost laying zinc strip.

When considering the results, the following phenomena should be considered which have a strong effect on the readings:

a) Response time of the equipment used to deter mine the "instant off" readings during the potential decay measurements.
b) Resistivities of the concrete and applied repair mortars.
c) Macrocell corrosion currents.
d) Anode to cathode surface areas.

One of the major issues encountered during potential decay measurements when using less appropriate equipment is the exact determination of the true "instant-off" potential reading. When a reference electrode is placed to measure the potential of the cathodically protected structure, this measurement will contain two components: (1) the steel-to-electrolyte potential and (2) the so-called IR-drop. The IR-drop error arises from the fact that current is flowing through the electrolyte and thus encounters an electrical resistance between the protected steel and the reference electrode.

This potential must be recorded quickly since the structure will start to depolarise immediately after switching-off the CP-current. According to the international code ISO 12696measurements of "instant off" are taken typically between 0.1s and 0.5s after switching "off" but it is mentioned that the appropriate time will vary from system to system and with the extent/period of polarisation.

Most of the equipment used in the field does not have the possibility to perform quick readings due to the low response time of the devices, like multimeters. A response time is the time required for achieving the accuracy specified for the corresponding range.

Potential readings during this experiment were performed with a Fluke 115 and Metrahit 23S multimeter. The first value appearing on the display of the multimeter immediately after switching off the CP current was considered to be the "instant off" potential.

A simple laboratory test was performed to determine the response time of the equipment so as to have an impression of the error arising from the use of less appropriate equipment for "instant off" readings. A CP system and a reference electrode were installed on a concrete specimen on which the IR-drop could be exactly determined by measuring the impedance of the reference electrode and multiplying the value with the measured CP current. For this particular set-up the IR-drop was determined at 13.3 mV.

An oscilloscope was used to measure the IR-drop value due to the very quick response times of oscilloscopes, however care should be taken because oscilloscopes can be very sensitive to noise.

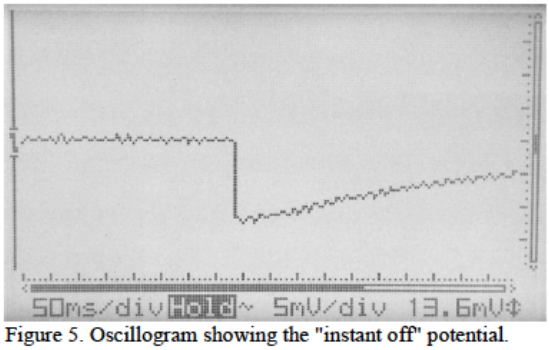

Figure 5. Oscillogram showing the "instant off" potential.

A total of 20 readings with the oscilloscope showed potential values between 13.6 and 29 mV.

Thereupon 3 multimeters, i.e. a Metrahit 23S, a Fluke 115, and a Fluke 287, were successively used to perform 12 "instant off" readings per device with the same CP lab set-up. Tables 5 to 7 provide an overview of the results.

Table 5, "instant off" readings from a Metrahit 23S meter

	Metrahit 23S		
	on	instant-off	
	mV	mV	δ mV
1	-625	-607	18
2	-625	-605	20
3	-625	-543	82
4	-625	-570	55
5	-625	-566	59
6	-625	-578	47
7	-625	-505	120
8	-626	-482	144
9	-627	-563	64
10	-627	-616	11
11	-627	-576	51
12	-627	-604	23
		Average =	58 mV
		SD =	41 mV

From these tables it can be seen that the IR-drop (δ mV) calculated from the "instant off" potential readings significantly differs from the true IR-drop (13.3mV). It can be concluded that the "instant off" potential readings obtained with these devices significantly overestimates the IR-drop values used to evaluate the cathodic protection system, which leads to an underestimation of the potential decay values. Despite the underestimation of the potential decay values, it shows that these devices are actually unsuitable for these kind of measurements performed on site.

Table 6, "instant off" readings from a Fluke 115 meter

	FLUKE 115		
	on	instant-off	
	mV	mV	δ mV
1	-637	-490	147
2	-637	-537	100
3	-637	-497	140
4	-637	-501	136
5	-637	-490	147
6	-637	-502	135
7	-637	-508	129
8	-637	-504	133
9	-637	-500	137
10	-637	-575	62
11	-637	-496	141
12	-637	-497	140
		Average =	129 mV
		SD =	24 mV

Table 7, "instant off" readings from a Fluke 287 meter

	FLUKE 287		
	on	instant-off	
	mV	mV	δ mV
1	-638	-547	91
2	-638	-483	155
3	-638	-613	25
4	-638	-492	146
5	-638	-502	136
6	-638	-583	55
7	-638	-514	124
8	-638	-488	150
9	-638	-493	145
10	-638	-491	147
11	-638	-481	157
12	-638	-497	141
		Average =	123 mV
		SD =	43 mV

Tables 1 and 2 show the direct relationship between the anode resistance and the current output. The resistances of each anode strip were measured with an LCR meter to avoid polarisation effects. Section 3 shows anode strips between nr A6 and A15 having relatively high resistances due to the mortar used for concrete repair.

The major part of the overall circuit resistance lies in the area in the immediate vicinity of the anode. The total grounding resistance of an anode, involves 3 components:

1. The resistance of the lead wire and the zinc anode itself, which usually is so small that it can be effectively discarded. However, in case of extended cable connections, the voltage drop in the wiring must be taken into account.
2. The transition resistance between the surface of the anode and the electrolyte is usually low. It can be increased by films of grease, paint, rust or deposits. It contains in addition an electrochemical polarisation resistance which depends on the magnitude of the current.
3. The grounding resistance which depends on both the magnitude of the current and the potential distribution in the electrolyte.

The resistivity of the repair mortar used, i.e. Weber.tc SBN 170, was measured in the laboratory and showed a strong increase of resistivity over time. After 360 days of aging the mortar reached a resistivity of nearly 12.000 Ohm·m. As a comparison: for wet portland cement concrete, resistivities will normally range from 50 to 200 Ohm·m whereas values between 500 and 4000 Ohm·m have been determined for blastfurnace slag concrete and for dry concrete. Usually the resistivities will vary over a wide range, depending on the temperature and moisture content.

An important consideration applies to achieving a uniform current density at the reinforcement steel within each anode zone, as current distribution on the concrete surface is governed by the concrete resistivity or repair mortar resistivity as stated in the RILEM TC154 Report. That is considered one of the reasons why international codes like ISO 12696 provide guidance on how to take into account variations in concrete resistivity. Therefore, for concrete repair the use of repair materials with an electrical resistivity within a range of approximately half to twice that of the parent concrete when measured under the same conditions as the parent concrete, is recommended. The resistivities of the repair mortars used have been determined and evaluated to identify possible effects by variations in the resistivities. Previous studies with galvanic anodes showed that the position of reference electrodes relative to the location of the anode can be critical when judging whether a system is performing well. These studies showed very clearly that potential decay readings were affected by the actively corroding bars located in close vicinity of the reference electrodes. The results also showed that the combination of passive and active bars embedded in close vicinity may produce a very high macrocell current resulting in such a strong polarisation that erroneous depolarisation readings may be obtained.

In many CP design recommendations and general literature on cathodic protection of steel structures and steel in concrete structures, anode/cathode surface area ratios, and limiting anode current densities are mentioned as points of particular interest due to the effect on the service life of anodes. Figure 7 shows the relationship between anode surface area and anode grounding resistance. It demonstrates that high anode surface areas facilitate higher current outputs. Wat is anode grounding resistance;

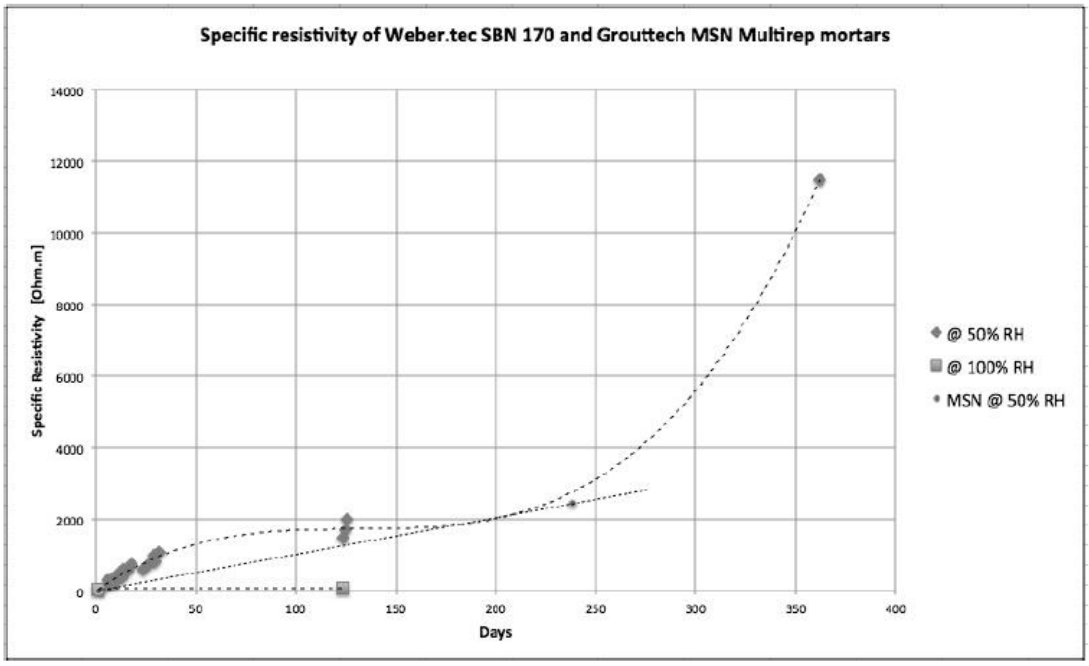

Figure 6. Progress of the resistivity over time of the 2 mortars used.

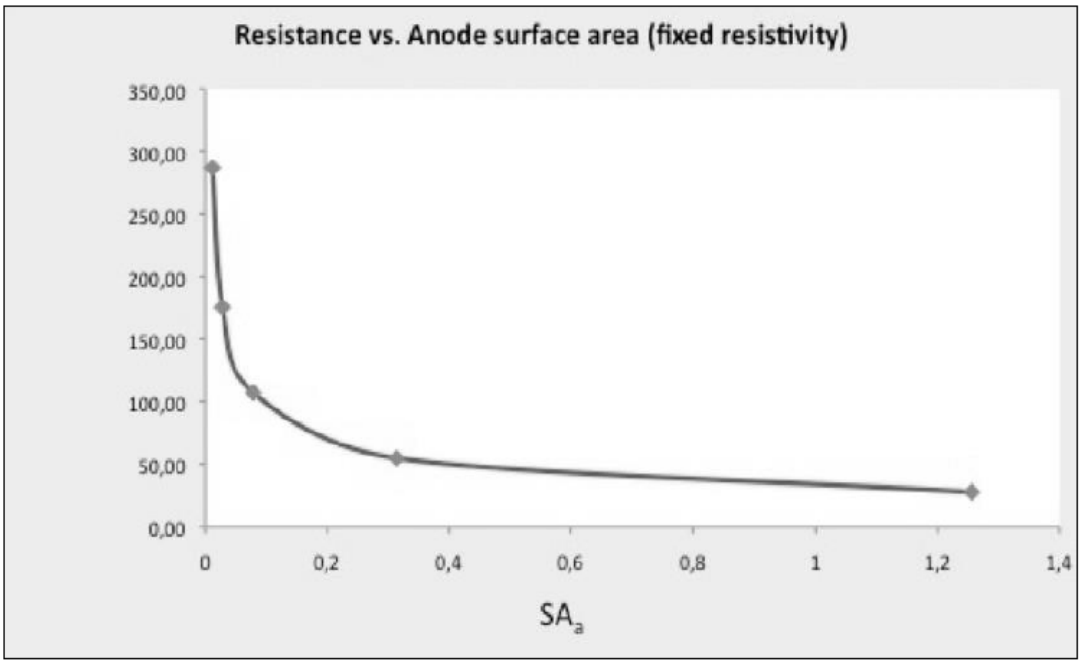

Figure 7. Graphic sketch of the theoretical relation between anode grounding resistance and anode surface area

.

The relation between anode resistance, current output, steel polarisation and anode/cathode surface area ratios concerning galvanic anodes is complex. This relation can only be explained in a qualitative way by using the "mixed potential theory". Figure 8 shows E-log I polarisation curves of an iron and a zinc electrode in an electrolyte. When electrically connected, the potential measured will be the point of intersection between the two curves and projected on the potential-axis which is the mixed potential of

the two electrodes. This type of diagram is inadequate to reflect all the effects of galvanic coupling, as it deals with current density, and therefore is not able to show the effects of different surface areas between anode and cathode.

Figure 9 is actually re-drawn by not using current density but total current on the log I-axis. This diagram is, however, able to show the effect of changing the area of one electrode relative to the other, and if the cathode area increases, the potential becomes less negative which means less polarisation of the structure, although with an increasing current output.

This phenomenon for sacrificial anodes with small anode dimensions applied on reinforced concrete structures is well noticed in the field. The small surface area of these sacrificial anodes are barely able to polarise the steel reinforcement of the concrete as their surface area is many times smaller than the surface area of the steel reinforcement. A simple solution to overcome this issue is to apply anodes with increased surface area.

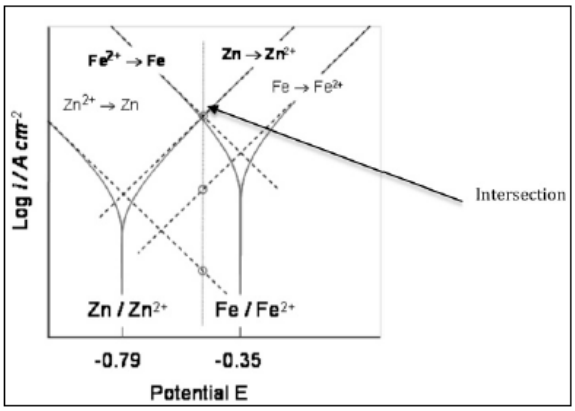

Figure 8. E-Log I polarisation curves of FE vs. Zn by using current densities.

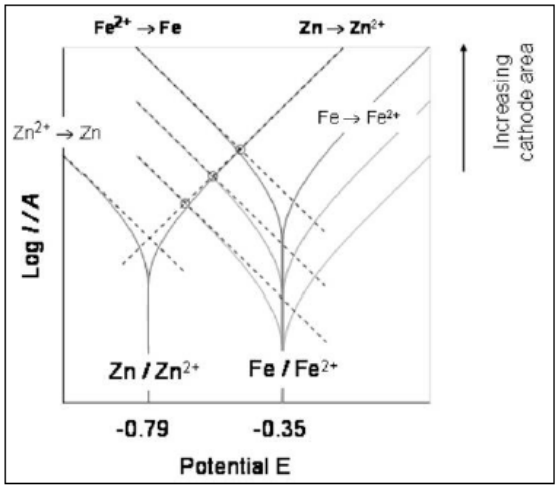

Figure 9. Theoretical E-log I polarisation curves of Fe vs. Zn by using total current output.

5 CONCLUSIONS

- Potential decay measurements show that for this specific situation the surface applied anode strips are able to polarise steel with a distance up to 60cm from the anode. Based on theoretical considerations the anode surface area will play an important role in the electric field distribution (throwing power) of galvanic anodes. Higher anode/cathode surface area ratios will increase the anode's "throwing power".

- Based on code based criteria, a distance of 10-20cm from the anode will give sufficient corrosion protection, given the fact that for this experiment readings were performed with equipment which strongly underestimates potential decay values.

- The use of repair mortars with low electric resistivities will improve the performance of galvanic anodes by increasing the current output and the anode's "throwing power".

6 REFERENCES

ISO/FDIS 12696:2011. Cathodic protection of steel in concrete.

Bruns, M. & Raupach, M. 2009. *CP of the rear reinforcement in RC-structures – Numerical modelling of the current distribution.* Concrete Repair, Rehabilitation and Retrofitting. 2nd International Conference on Concrete Repair, ICCRRR-2, Nov. 2008, Cape Town, South Africa, M.G Alexander, H. Beushausen, F.Dehn and P. Moyo (Eds) CRC Press 2008, Pages 301–302

Baeckmann, W. von & Schwenk, W. Handbook of Cathodic Corrosion Protection. *Distribution of current and potential in a stationary electric field*. Elsevier, 1997

Giorgini, R. 2014. *Issues using potential decay techniques to asess a cathodic protection system of steel in concrete caused by macrocell corrosion*. Proceedings of Concrete Solutions 2014, 5th International Conference on Concrete Repair, Belfast. CRC Press, 2014

Giorgini. R. & Papworth, F. 2011. code based protection Galvanic cathodic protection system complying with criteria. Accessed from http://www.srcp.com.au/images/pdf/03-cia-galvanic-anodes.pdf March 2016

Kelly, R.G, Scully, John R., Shoesmith, D and Bucheit Rudolph G. *Electrochemical Techniques in Corrosion Science and Engineering* 2002, CRC Press

RILEM TC154-EMC.2003, *Electrochemical techniques for measuring metallic corrosion*. RILEM Publications Sarl.